

## Fault and damage pro-elasticity model in multi-plane framework for rocks

S. A. Sadrnejad<sup>1,\*</sup>, M. Nikbakhsh zati<sup>2</sup>, M. Memarianfard<sup>3</sup>

Received: February 2009, Accepted: May 2010

### Abstract

*An important concern in rock mechanics is non-homogeneity as joints or fault. This noticeable feature of failures in rock is appearance of slip surfaces or shear bands, the characteristics of that are associated with deformation being concentrated in a narrow zones and the surrounding material remaining intact. Adopting the joints as fractures, fractures are well known for their effects on the mechanical and transport properties of rock. A damaged pro-elasticity multi-plane based model has been developed and presented to predict rock behavior. In this multi-plane model, the stress-strain behavior of a material is obtained by integrating the mechanical response of an infinite number of predefined oriented planes passing through a material point. Essential features such as the pro-elasticity hypothesis and multi-plane model are discussed. The methodology to be discussed here is modeling of slip on the local and global levels due to the deformation procedure of the existing/probable joints of rock and this method has a potential of using different parameters on different sampling planes to predict inherent anisotropy of rocks. Upon the presented methodology, more attention has been given to slip initiation and propagation through these joints. In particular, softening in non-linear behavior of joints in going from the peak to residual strengths imparts a behavior often associated with progressive failure. The predictions of the derived stress-strain model are compared to experimental results for marble, sandstone, Quartz mica schist and anisotropic schist. The comparisons demonstrate the capability of this model to reproduce accurately the mechanical behavior of rocks.*

*Keywords: Multi-plane model, Pro-elasticity, Damage, Pre-failure mechanism, Pre-failure mechanism.*

### 1. Introduction

It is known that the mechanical behavior of rocks generally is elasto-plastic, dilatants, strain hardening and strain softening. The identification of the post-peak behavior of rocks, in which the strain-softening or strain hardening occurs, under various confinement pressure is time-consuming and need to utilizing a special set up. Hence, the various elasto-plastic constitutive models based on the associated or non-associated flow rules developed for this purpose [1-6]. It is to be note that, the using of these models is intricate and need to various parameters for applicability in the prediction of mechanical behavior of rocks.

The vertical joints in sedimentary rocks that occur through a

wide range spectrum of tectonic environments have puzzled investigators since the early days of geo-mechanics. The orientation of joints was correlated with strikes of the latter day faulting and cracks, as well as with old basement fractures. From the finite elements boundary condition point of view the discontinuities in a rock mass is classified in two categories as: discontinuities with and without in filled gouge materials. The first category includes major discontinuities like faults, crushed or sheared zones. However, when the thickness of the infilling material is more than about twice the height of asperities, the strength and deformability of the discontinuity is governed by those of the infilling material. Such discontinuities produce regions of non-homogeneity that must conform to the fault or crushed zones boundaries. The material model adapted to model discontinuities would depend on the mechanical behavior of gouge material. The second category of discontinuities (without in filled gauge material) generally form a kind of fabric. In analysis of such discontinuities, it is assumed to be ubiquitous and the stress-strain constitutive laws for the rock must be modified to take the fabric of discontinuities into account.

\* Corresponding Author: [sadrnejad@kntu.ac.ir](mailto:sadrnejad@kntu.ac.ir)

<sup>1</sup> Professor of Department of Civil Engineering, K.N.Toosi University of Technology, Tehran

<sup>2</sup> Ph.D. Candidate, Department of Civil Engineering, K.N.Toosi University of Technology, Tehran

<sup>3</sup> Post Doc. Student, Department of Civil Engineering, K.N.Toosi University of Technology, Tehran

A noticeable feature of rock media failures is the appearance of slip surfaces or shear band, the characteristics of that are associated with deformation being concentrated in narrow zones and the surrounding material remaining intact. The concept of a distinct failure plane that forms a wedge of material allows a direct examination of force equilibrium of the system and is central to most stability calculation. This problem includes a certain behavior of a local joint in global level due to the development of sliding and shear band. The softening observed in going from peak to residual strengths imparts a behavior often associated with progressive failure.

Also, many experimental laboratory studies, particularly those carried out on solid rock cylinders under axisymmetric compressive stress conditions, have led to a substantial amount of knowledge regarding the anisotropic behavior of stratified (bedded, laminated, foliated, schistose) rocks. There is a considerable body of experimental work which shows that anisotropy may control the geometry of rock deformation.

However, in axisymmetric tests it is not possible to determine the effect of either the magnitude, or the orientation of the intermediate principal stress on the behavior of anisotropic rocks. In particular, the dependence of fault orientation on the magnitude and sense of intermediate stress cannot be determined.

Research was undertaken here, with the aim of gaining a better understanding of the effect of intermediate principal stress on the behavior of anisotropic rocks. Rectangular prismatic samples of anisotropic foliated crystalline schist, differently oriented with respect to the directions of the applied principal stresses, were tested under conditions of a true or general triaxial compression. A set of investigations of the behavior of rocks with planar anisotropy under true triaxial stress conditions (Mogi et al- 1978) [7] was built upon the pioneer Mogi's work on prismatic, rectangular samples of quasi-isotropic rocks.

Any fault or joint slip manifested as rock-bursts is imparted in global response by corresponding constitutive equations and a number of parameters being carried out through calibrating test results. Therefore, all non-homogeneity characteristic responses through a typical joint imparts through the calculated behavioral matrix presented for sliding and closing/widening characteristics. A similar set of parameters were developed to characterize this dynamic process as the fundamental quantity called the moment tensor (Aki and Richard 1980) [8]. The continuously yielding model developed by Cundal & Hart, 1984[9], simulates the behavior of rock joint in a simple manner upon the internal mechanism of progressive damage of joints under shearing. This model could be more realistic as it considers the non-linear behavior observed in physical tests such as joint material degradation, normal stiffness, dependence on normal stress, and the change in dilation rate with plastic shear displacement[20,31,32].

The multi-plane developed by Sadrnejad, (2005,2006)[10, 11], is capable of predicting the behavior of geo-materials such as rock on the basis of sliding mechanisms, elastic behavior of intact parts and possibilities to see different plasticity models for the most possible sliding orientations. The influences of rotation of the direction of principal stress and strain axes and induced/inherent anisotropy are included in a rational way

without any additional hypotheses. The spatial strength distribution at a location as an approximation of probable mobilized sliding mechanism is proposed as an ellipsoid function built up on bedding plane.

According to the proposed model, the interface asperity shapes that is identical to model based on the minimum energy level, identify the active sliding orientations, cracks, and joints. Furthermore, the sliding behavior of any predefined existing joints through the rock mass is introduced to the matrix of global mechanical behavior based on a realistic and logical way.

## 2. Strain distribution around a point

In general continuum mechanics, to define strain distribution at a point, the components are simply considered on the outer surface of a typical  $dx, dy, dz$  element. This method makes the solution to be considered uniform and the homogeneous strain distribution of the nine components over the outer surface of such  $dx, dy, dz$  element on three perpendicular coordinate axes. There is a further consideration in addition to the requirement that the displacements of a cemented or granular medium provide due to slippage/widening/closing between particles that make a contribution to the strain in addition to that from the compression of particles. Consider two neighboring points on either side of the point of contact of two particles. These two points do not in usual remain close to each other but describe complex trajectories. Fictitious average points belonging to the fictitious continuous medium can be defined which remain adjacent so as to define a strain tensor. The problem presents itself differently for disordered particles compared with the ordered sphere of equal sizes. In this case, small zones may even appear in which there is no relative movement of particles. This can lead to specific behavior such as periodic instabilities known as slip-stick, creating non-homogeneity in strains and displacements. The effects of non-homogeneity in the mechanical behavior of non-linear materials are very important and must somehow be considered. Furthermore, these non-homogeneities are mostly neglected in mechanical testing because strains and stresses are usually measured at the boundary of the samples and therefore have to be considered reasonably within the whole volume. Solving non-linear problems, the mechanical behavior depends strongly on the stress/strain path as well as their histories. Upon these conditions, it may be claimed that the consideration of strain components along three perpendicular coordinate axes may not reflect the real historical changes during the loading procedure. In the most extreme case, the definition of a sphere shape element  $dr$  (instead of  $dx, dy, dz$  cube) carrying distributed strain similarly on its surface can reflect strain components on infinite orientation at a point when  $dr$  tends to zero.

The finite strain at any point in three dimensions by coordinates  $(x, y, \text{ and } z)$  relates to the displacements of the sides of an initial rectangular-coordinate box with sides of length  $dx, dy, \text{ and } dz$  to form the three sides of a parallelepiped. This configuration of strain is established by considering the displacements of the corner points  $(x, 0, 0), (0, y, 0), \text{ and } (0, 0, z)$ . This kind of strain approach leads to defining a  $(3 \times 3)$  strain tensor including six components to present the displacement gradient matrix at a node.

Accordingly, any displacement and corresponding gradient have to be defined as independent components on three perpendicular coordinate axes.

Figure 1 shows sphere elements and typical deformed shapes for joint less and jointed elements. Obviously there is a certain history of displacement on any random orientation through the elements. These are abbreviated in only three  $x$ ,  $y$  and  $z$  planes, when a box - shape  $dx dy dz$  element is employed. To avoid not missing any directional historical information of strains, a spherical element carrying strain components over its surface as tangent and normal to the surface must be employed. This form of strain, which certainly represents a better distribution, includes all directional information. Certainly, to obtain the strain components as presented on planes around box element, strain variation is integrated over the sphere surface. However, a predefined numerical integration may be employed to ease the solution.

Numerical integration generally simulates the smooth curved sphere surface to a composition of flat tangential planes, making an approximated polygon to sphere surface. The higher the number of sampling planes, the closer is the approximated surface to the sphere. Clearly, if the number of sampling planes is taken as six, the approximated surface is the same as the normal  $dx dy dz$  box element [32-35].

### 3. Damage Multi-plane model for rock

The basic concept that a number of slip planes contribute to plastic flow was first proposed by Batdorf and Budiansky [12] in the context of polycrystalline materials and was extended to clays by Calladine [13]. Conceptually, the idea was already discussed by Taylor [14]. A constitutive model for jointed rock masses having a finite set of parallel planes of weakness was first proposed by Zienkiewicz and Pande [15]. Assuming that soils have an infinite number of randomly oriented sets of planes, the soil model was extended by Pande and Sharma [16] for clays and by Sadrnejad and Pande [17] for sands. MMS was developed and implemented in the commercially available finite element code Plaxis [18] by Wiltafsky [19] as a user-defined soil model. It was extended by Scharinger and Schweiger [20, 26] to include small strain stiffness effects.

For an employed numerical integration rule and the calculation of a stress tensor of each plane are shown in Figure 2. Upon yield criterion in plasticity, the stress condition exceeds the yield limits, plastic sliding or widening/closing take place as an active plane. Therefore, one of the most important features of a multi-plane framework is that it enables the identification of the active

planes as a matter of routine. The application of any stress path is accompanied by the activities of some of the 13 defined planes at any point in the medium. The values of plastic/softening/crack initiation with large strain on all the active planes are not necessarily the same. Some of these planes initiate such plastic deformations earlier than others. These priorities and certain active planes can change due to any change of direction of the stress path. A number of active planes may stop activity or closing the initiated crack up, while some inactive ones become active, and some planes may take over others with respect to the value of the plastic strain. Thus the framework is able to predict the mechanism of failure. We use multi-plane framework for prediction of the non-linearity behavior of rocks in this article.

The orientation of a sampling plane or micro-plane is characterized by the unit normal  $n$  of components  $n_i$  (indices  $i$  and  $j$  refer to the components in Cartesian coordinates  $x_i$ ). In the formulation with a kinematic constraint, which makes it possible to describe softening behavior of plane concrete in a stable manner, the strain vector  $\vec{\epsilon}_N$  on the micro-plane (Figure 2) is the projection of the macroscopic strain tensor  $\epsilon_{ij}$ . So the components of this vector are  $\epsilon_{Ni} = \epsilon_{ij} n_j$ . The normal strain on the micro-plane is  $\epsilon_N = n_i \epsilon_{Ni}$ , that is

$$\epsilon_N = N_{ij} \epsilon_{Ni} ; N_{ij} = n_i n_j \quad (1)$$

Where repeated indices imply summation over  $i=1,2,3$ . The mean normal strain, called the volumetric strain  $\epsilon_V$ , and the deviatoric strain  $\epsilon_D$  on the micro-plane can also be introduced, defined as follows:

$$\epsilon_V = \epsilon_{KK} / 3 ; \quad \epsilon_D = \epsilon_N - \epsilon_V \quad (2)$$

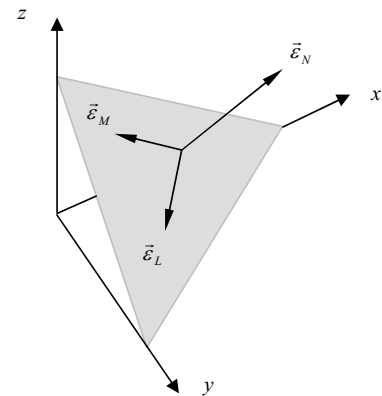


Fig. 2. Strain components on a micro-plane

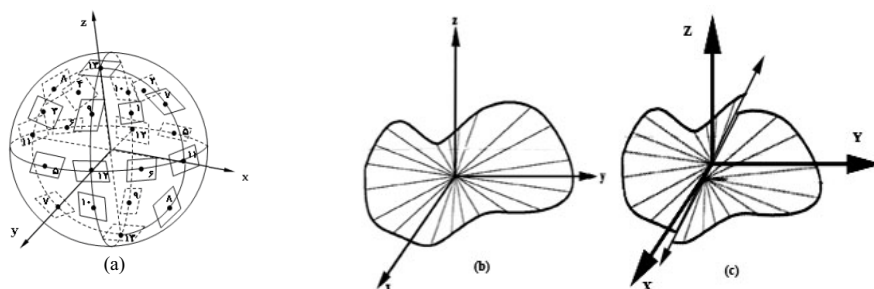


Fig. 1. a- isotropic sphere elements, b- deformed element, c-deformed jointed element

This separation of  $\varepsilon_V$  and  $\varepsilon_D$  is useful when the effect of the hydrostatic pressure for a number of cohesive frictional materials, such as concrete, needs to be captured. To characterize the shear strains on the micro-plane (Figure 3), we need to define two coordinate directions  $M$  and  $L$ , given by two orthogonal unit coordinate vectors  $m$  and  $l$  of components  $m_i$  and  $l_i$  lying on the micro-plane. To minimize directional bias of  $m$  and  $l$  among micro-planes, one of the unit vectors  $m$  and  $l$  tangential to the plane is considered to be horizontal (parallel to  $x$ - $y$  plane).

The value of the shear strain components on the micro-plane in the direction of  $m$  and  $l$  are  $\varepsilon_M = m_i(\varepsilon_{ij} n_j)$  and  $\varepsilon_L = l_i(\varepsilon_{ij} n_j)$ . Because of the symmetry of tensor  $\varepsilon_{ij}$ , the shear strain components may be written as follows (e.g. Bažant et al., 1985, 1988) [21, 22]:

$$\varepsilon_M = M_{ij} \varepsilon_{ij} ; \quad \varepsilon_L = L_{ij} \varepsilon_{ij} \quad (3)$$

In which the following symmetry tensors were introduced:

$$M_{ij} = (m_i n_j + m_j n_i) / 2 ; \quad L_{ij} = (l_i n_j + l_j n_i) / 2 \quad (4)$$

Once the strain components on each micro-plane are obtained, the stress components are updated through micro-plane constitutive laws, which can be expressed in algebraic or differential forms. In the kinematic constraint micro-plane models, the stress components on the micro-planes are equal to the projections of the macroscopic stress tensor  $\sigma_{ij}$  only in some particular cases, when the micro-plane constitutive laws are specifically prescribed in a manner such that this condition can be satisfied.

This happens for example in the case of elastic laws at the micro-plane level, defined with elastic constants chosen so that the overall macroscopic behavior is the usual elastic behavior (Carol and Bažant, 2001) [23]. In general, the stress components determined independently on the various micro-planes will not be related to one another in such a manner that they can be considered as projections of a macroscopic stress tensor. Thus the static equivalence or equilibrium between the micro level stress components and macro level stress tensor must be enforced by other means. This can be accomplished (as proposed in Bažant, 2004) [24] by application of the principle of virtual work, yielding

$$\sigma_{ij} = \sigma_V \delta_{ij} + \frac{3}{2\pi} \int_{\Omega} \left[ \sigma_D \left( N_{ij} - \frac{\delta_{ij}}{3} \right) + \sigma_L L_{ij} + \sigma_M M_{ij} \right] d\Omega \quad (5)$$

Where  $\Omega$  is the surface of a unit hemisphere,  $\sigma_V$  and  $\sigma_D$  are the volumetric and deviatoric part of normal stress component and  $\sigma_L$  and  $\sigma_M$  are as shear stress components on the micro-planes respectively. Equation (5) is based on the equality of the virtual work inside a unit sphere and on its surface, rigorously justified by Bažant et al. 2004[24].

The integration in equation (5) is performed numerically by Gaussian integration using a finite number of integration points on the surface of the hemisphere. Such an integration technique corresponds to considering a finite number of micro-planes, one for each integration point. An approximate formula consisting of 26 integration points is proposed in this study. In the table 1, direction cosines and weights of the integration points and presented in Figure 3. The use of this numerical integration technique for evaluation of integral statement in equation (5) yields:

$$D_{ijkl} = \frac{3}{4\pi} \int_{\Omega} \left( \frac{E}{1+\nu} \right) \left[ \left( N_{ij} - \frac{\delta_{ij}}{3} \right) \left( N_{kl} - \frac{\delta_{kl}}{3} \right) + M_{ij} M_{kl} + L_{ij} L_{kl} \right] d\Omega + \frac{E}{1-2\nu} \frac{\delta_{kl}}{3} \delta_{ij} \quad (6)$$

$N_m$  is the number of integration points on hemisphere. Based on The formulation, macroscopic constitutive matrix in the proposed model is obtained as follows:

$$D_{ijkl} = \frac{3}{4\pi} \int_{\Omega} \left( \frac{E}{1+\nu} \right) \left[ \left( N_{ij} - \frac{\delta_{ij}}{3} \right) \left( N_{kl} - \frac{\delta_{kl}}{3} \right) + M_{ij} M_{kl} + L_{ij} L_{kl} \right] d\Omega + \frac{E}{1-2\nu} \frac{\delta_{kl}}{3} \delta_{ij} \quad (7)$$

$E$  and  $\nu$  are as elastic modulus and Poisson's coefficient.

#### 4. Proposed Damage Function Formulation

Total deviatoric part of constitutive matrices is computed from superposition of its counterparts on the micro-planes that such counterparts in turn, are calculated based on the damages occurred on each plane depending on its specific loading conditions [14].

This damage is evaluated according to the five separate damage functions; each of them belongs to the particular loading states. This five loading conditions are as follows:

1. hydrostatic compression
2. hydrostatic extension
3. pure shear
4. shear + compression
5. shear + extension

On each micro-plane at each time of loading history, there exists one specific loading situation that it may be in one of the

Plane NO	1	2	3	4	5	6	7	8	9	10	11	12	13
NORMAL AXIS	$l_i$	$\frac{\sqrt{3}}{3}$	$\frac{\sqrt{3}}{3}$	$-\frac{\sqrt{3}}{3}$	$-\frac{\sqrt{3}}{3}$	$\frac{\sqrt{2}}{2}$	$-\frac{\sqrt{2}}{2}$	$\frac{\sqrt{2}}{2}$	$-\frac{\sqrt{2}}{2}$	0	0	1	0
	$m_i$	$\frac{\sqrt{3}}{3}$	$-\frac{\sqrt{3}}{3}$	$\frac{\sqrt{3}}{3}$	$-\frac{\sqrt{3}}{3}$	$\frac{\sqrt{2}}{2}$	$\frac{\sqrt{2}}{2}$	0	0	$-\frac{\sqrt{2}}{2}$	$\frac{\sqrt{2}}{2}$	0	1
	$n_i$	$\frac{\sqrt{3}}{3}$	$\frac{\sqrt{3}}{3}$	$\frac{\sqrt{3}}{3}$	$\frac{\sqrt{3}}{3}$	0	0	$\frac{\sqrt{2}}{2}$	$\frac{\sqrt{2}}{2}$	$\frac{\sqrt{2}}{2}$	$\frac{\sqrt{2}}{2}$	0	0
$W_i$		$\frac{27}{840}$	$\frac{27}{840}$	$\frac{27}{840}$	$\frac{27}{840}$	$\frac{32}{840}$	$\frac{32}{840}$	$\frac{32}{840}$	$\frac{32}{840}$	$\frac{32}{840}$	$\frac{32}{840}$	$\frac{40}{840}$	$\frac{40}{840}$
		$\frac{840}{840}$	$\frac{840}{840}$	$\frac{840}{840}$	$\frac{840}{840}$	$\frac{840}{840}$	$\frac{840}{840}$	$\frac{840}{840}$	$\frac{840}{840}$	$\frac{840}{840}$	$\frac{840}{840}$	$\frac{840}{840}$	$\frac{840}{840}$



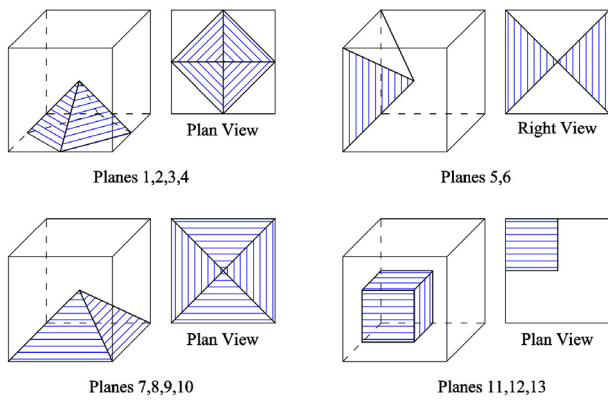


**Fig. 3.** Direction cosines, weighted coefficient, demonstration of 13 planes

five mentioned basic loading conditions. For every five mood, a specific damage function according to the authoritative laboratory test results available in the literature is assigned. Then, for each state of on plane loading, one of the five introduced damage functions will be computed with respect to the history of micro-stress and strain components. These five damage functions are as below:

$$\omega_{HC} = 0.0 \quad (8)$$

$$\begin{cases} \omega_{HT} = 0.0 & \text{if } \varepsilon_{eq} \leq \sqrt{3}a \\ \omega_{HT} = 1.0 - \left( \frac{\sqrt{3}a}{\varepsilon_{eq}} \right) \times \exp \left[ - \left( \frac{\varepsilon_{eq} - \sqrt{3}a}{b - \sqrt{3}a} \right) \right] & \text{if } \varepsilon_{eq} > \sqrt{3}a \end{cases}$$

$$\omega_{SH} = 0.5 \times (\omega_C + \omega_T) \quad (10)$$

$$\begin{cases} \omega_C = d \times \varepsilon_{eq} & \text{if } \varepsilon_{eq} \leq e \\ \omega_C = f(\varepsilon_{eq} - e)^2 + g(\varepsilon_{eq} - e) + h & \text{if } e < \varepsilon_{eq} \leq i \\ \omega_C = 1.0 - \left( \frac{j}{\varepsilon_{eq}} \right) \times \exp \left[ - \left( \frac{\varepsilon_{eq} - i}{k - i} \right) \right] & \text{if } \varepsilon_{eq} > i \end{cases} \quad (11)$$

$$\begin{cases} \omega_T = 0.0 & \text{if } \varepsilon_{eq} \leq a \\ \omega_T = 1.0 - \left( \frac{a}{\varepsilon_{eq}} \right) \times \exp \left[ - \left( \frac{\varepsilon_{eq} - a}{c - a} \right) \right] & \text{if } \varepsilon_{eq} > a \end{cases} \quad (12)$$

Parameters  $a$  to  $k$  in the above relations are computed according to laboratory results obtained for each specific rock. In equation (9),  $\varepsilon_{eq}$  is as average strain and in the other relations is as the magnitude of projected deviatoric strain vector on each micro-plane.

## 5. Verification of model results

To present the ability of the proposed model, the tri-axial test results conducted on Marble, sandstone and Quartz mica schist are produced by the model. The prediction of the model for elasto-Plastic behavior of marble has been compared with test results. Figure 5a, b shows the comparison of the model result with standard triaxial tests for marble as stress deviator versus axial strain. Also, the comparison of volumetric strain versus axial strain are shown in Figure 6a, b.

From the comparison between these Figures, the ability of the model to reproduce the main features of the marble behavior has been demonstrated.

## 6. Elasto-Plastic behavior of sandstone

Figure 7a, b shows the comparison of the model result with tri-axial tests for sandstone as stress deviator versus axial strain. Also, the comparison of stress deviator versus lateral strain are shown in Figure 8a, b.

## 7. Elasto-Plastic behavior of Quartz mica schist

To show the capability of the proposed model in predicting the softening behavior, the tri-axial test results presented by Varadarajan, et al. [25], [31] were produced and compared with the test results. Figure 10a, b shows the comparison of the model result with tri-axial tests for Quartz mica schist as stress

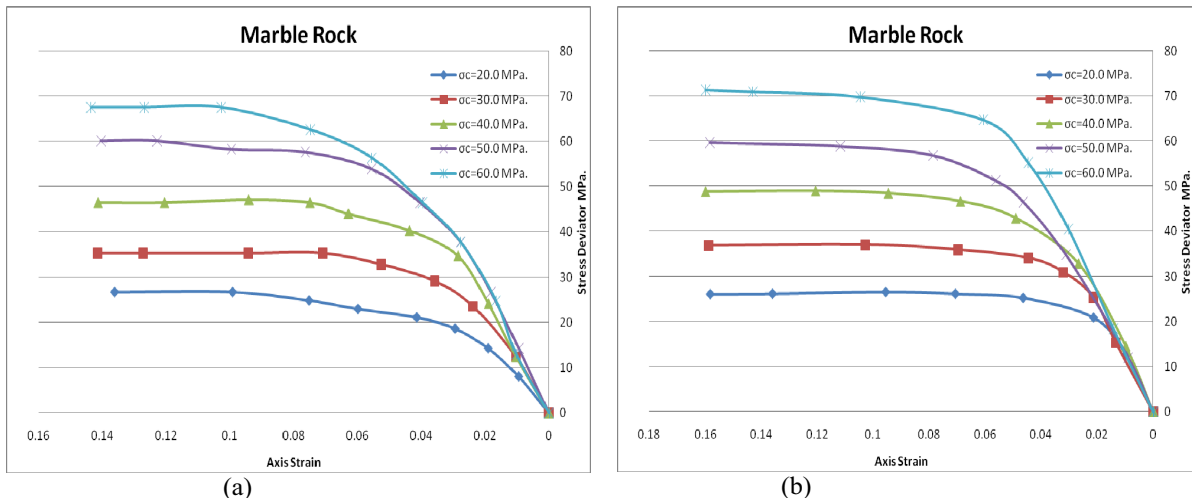


**Fig. 5.** Comparison of experimental with model results for marble (different confining stress); a) test results, b) model results

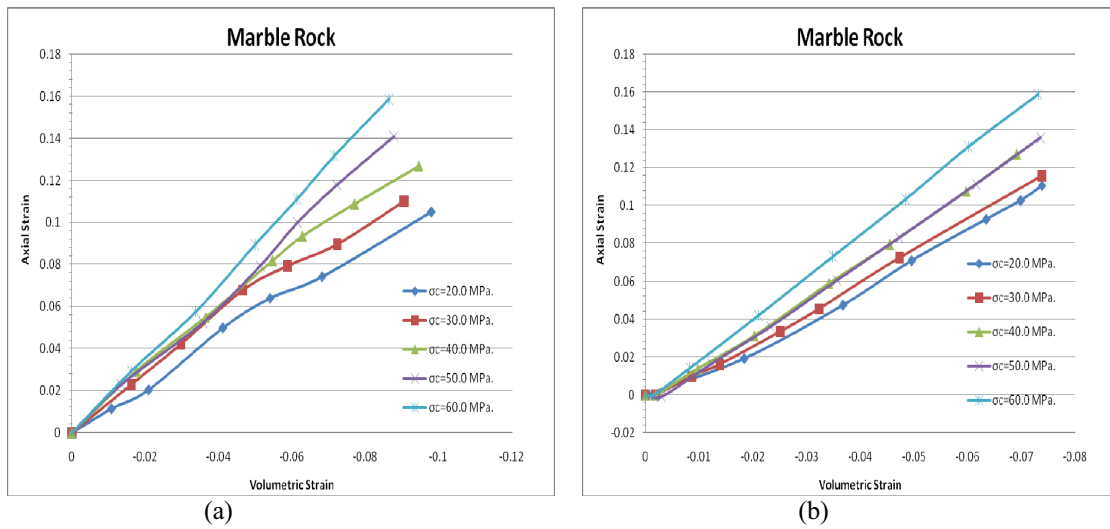


Fig. 6. Comparison of experimental with model results for marble (different confining stress); a) test results, b) model results.

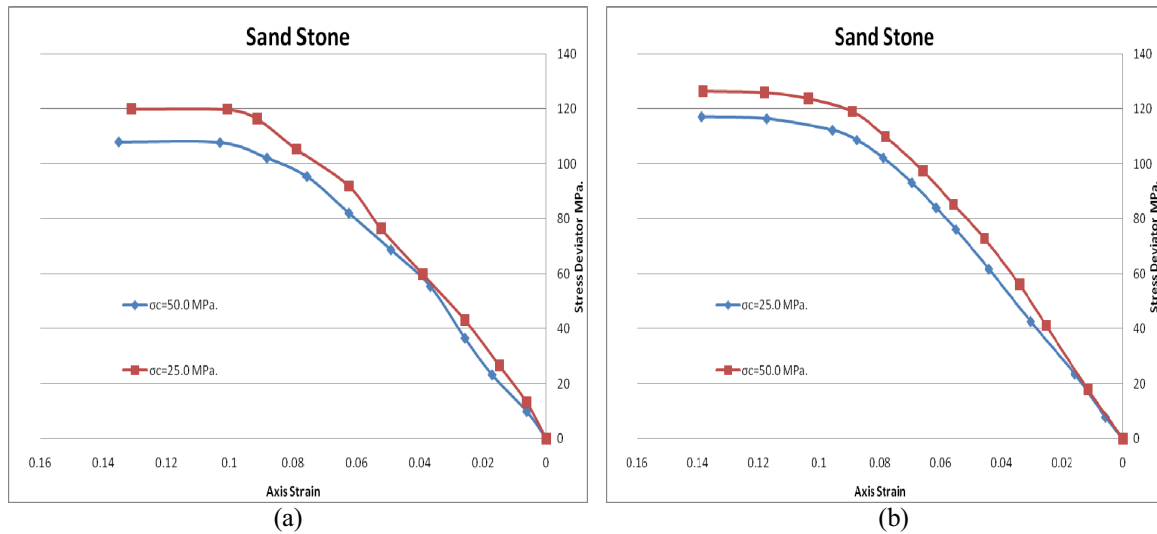


Fig. 7. Comparison of experimental with model results for sandstone (different confining stress): (a) test results; and (b) model results

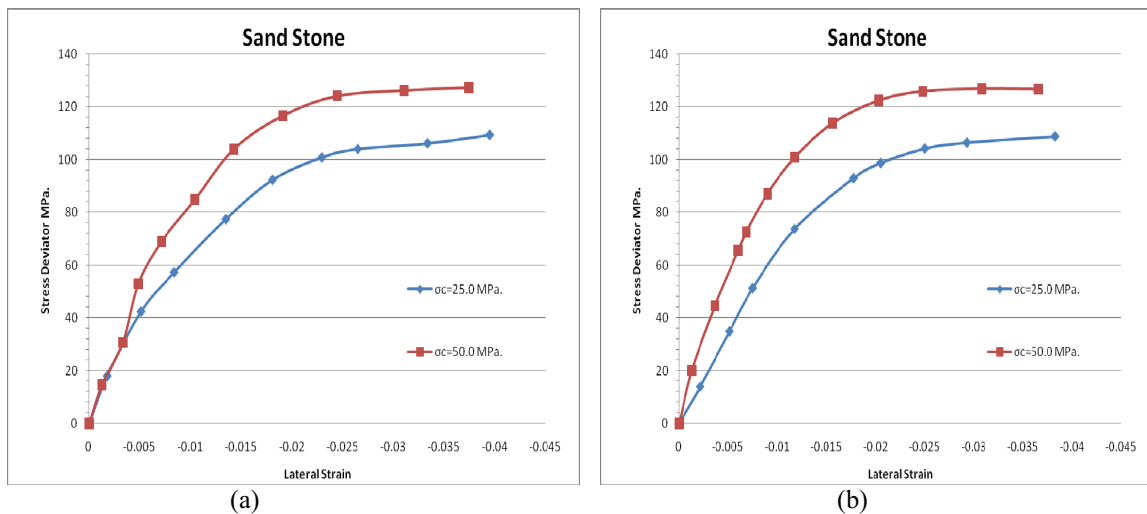


Fig. 8. Comparison of experimental with model results for sandstone (different confining stress): (a) test results; and (b) model results.

deviator versus axial strain. Also, the comparison of stress deviator versus lateral strain are shown in Figure 10a, b. The model predicts a strain-softening phenomenon as it assumed, also a good accuracy was obtained between numerical simulations and experimental results.

## 8. The effects of bedding plane on the orientation of planar shear stress

To show the capability of the proposed model in predicting the effects of bedding plane and changes in the orientation of on plane shear stresses upon the certain stress path in true triaxial test, presented by Kwasniewski & Mogi 1990, [27] were predicted and compared with the experimental results. Rectangular prismatic samples of a metamorphic, green crystalline schist were tested under conditions of a true triaxial homogeneous state of compressive stresses ( $\sigma_1 > \sigma_2 > \sigma_3$ ). The samples were loaded in such a way that the maximum principal stress ( $\sigma_1$ ) was oriented at angle  $\beta=90^\circ$  to the

foliation planes (which is the direction of the highest compressive strength), or at angle  $\beta=30^\circ$  (direction of the lowest compressive strength). In the latter case the samples were oriented such that the angle ( $\omega$ ) between the direction of the intermediate principal stress ( $\sigma_2$ ) and the strike of the plane of foliation was  $0^\circ$ ,  $45^\circ$  or  $90^\circ$ . Figure 11 shows the direction of principal stress axes and bedding plane orientations for four set of tests.

Results of the study represent a new light on the phenomenon of faulting under true three-dimensional stress conditions. They show that in stratified geologic media it might not necessarily be true that the plane of fracture (faulting) is parallel to the direction of the intermediate stress (as normally is the case in massive or isotropic rock masses). However, these are the weakness planes which may control the geometry of rock deformation and faulting. It has also been revealed that seismic or seismic faulting may take place in stratified rock masses depending on the major and the intermediate principal stress orientation relative to the planes of weakness.

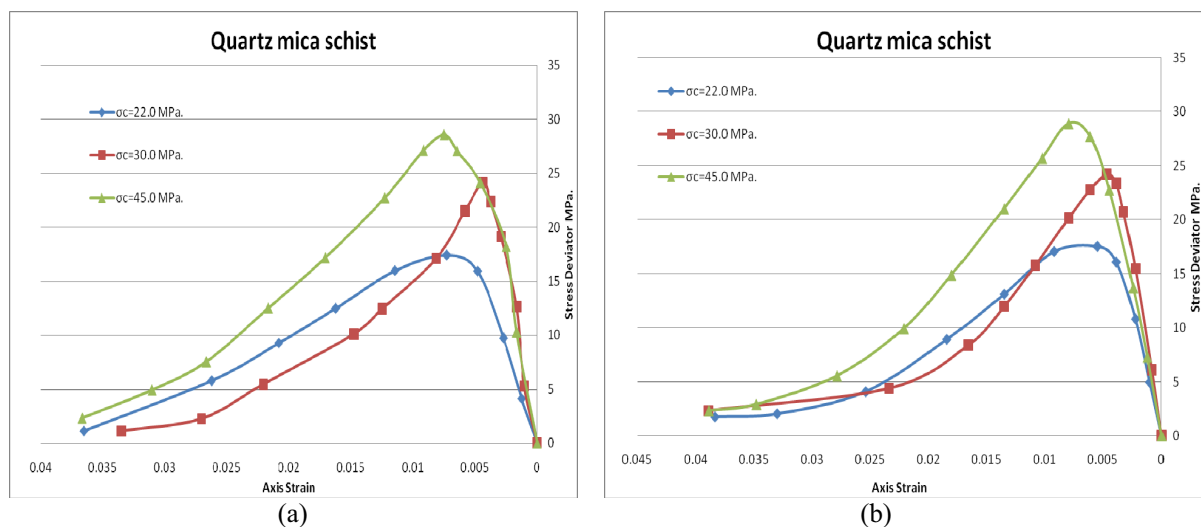


Fig. 9. Comparison of experimental with model results for Quartz mica schist (different confining stress): (a) test results; and (b) model results

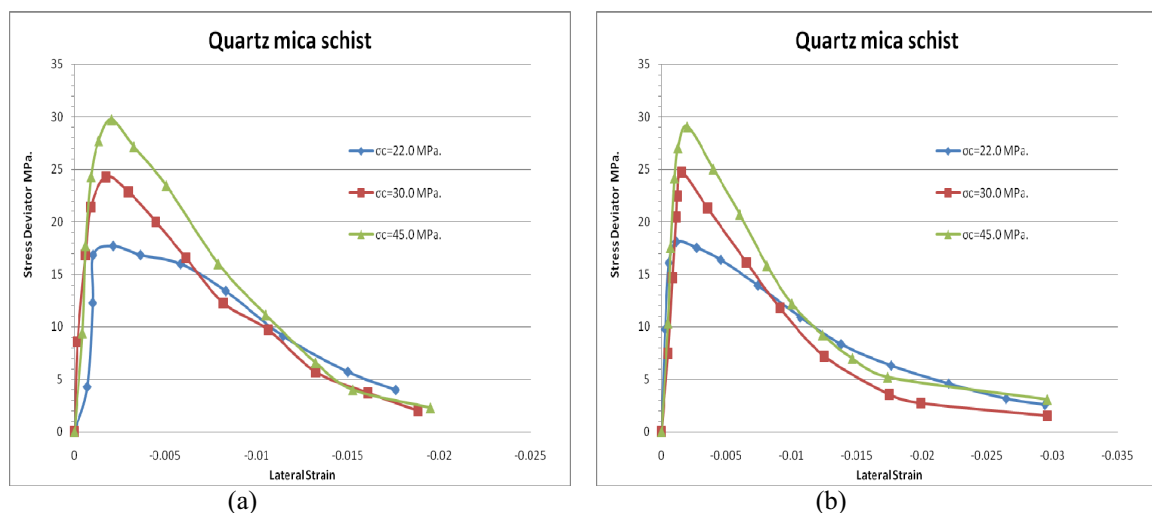


Fig. 10. Comparison of experimental with model results for Quartz mica schist (different confining stress): (a) test results; and (b) model result.

Figure 12 shows different stress-strain curves based on the changes of principal stress axis and bedding plane orientations. Figure 13, 14 and 15 show the comparison of stress deviators versus axial strains at the various ( $\sigma_2$ ) values of the conducted true triaxial tests on rock samples upon three sets of changes of applied stresses with regards to bedding plane orientations. The objective of these tests were to investigate and show the

mode of failure and the pattern of faults developed in samples of an anisotropic rock as the changes of shear stress orientation on active sliding planes in a general triaxial stress field.

Special attention will be paid to the effect of the intermediate principal stress on the faulting and associated phenomena. Macroscopically homogeneous green crystalline schist with a distinct, dense foliation was selected for the studies. This was

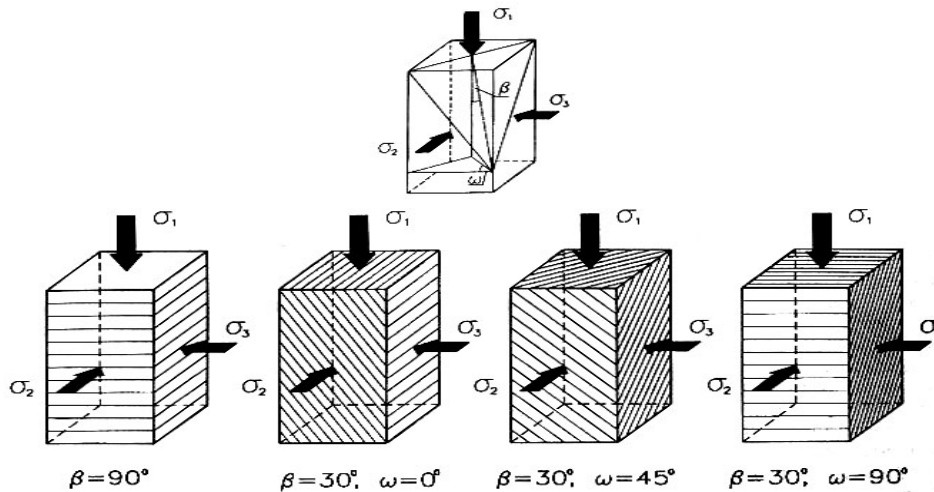


Fig. 11. Four different orientations of bedding plane of the rock samples ( $\omega$ ) and stresses ( $\sigma_1 > \sigma_2 > \sigma_3$ )

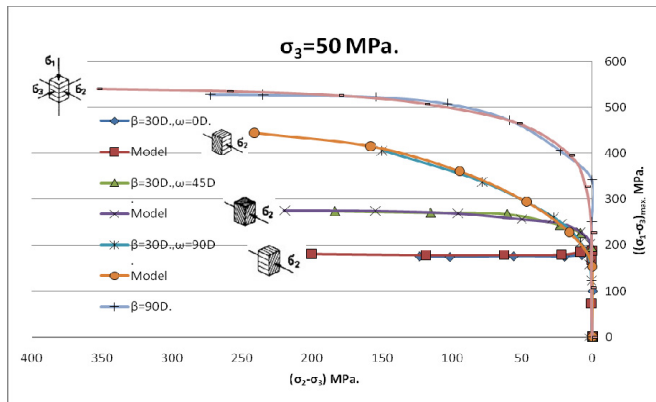


Fig. 12. Stress deviators variations on two perpendicular planes of Chichibu schist for different orientations of bedding planes (Kwasniewski & Mogi 1996) [ 28]

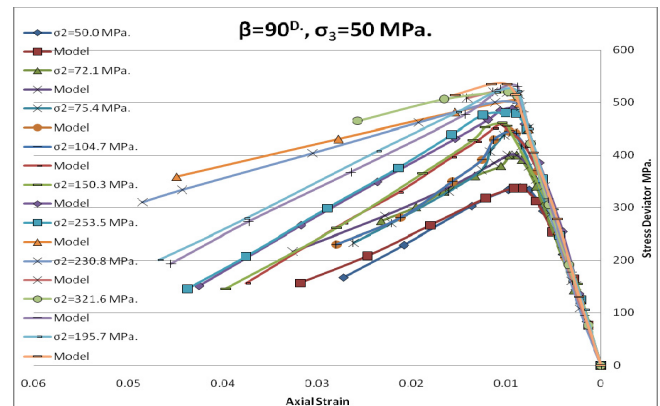


Fig. 14. Stress deviator versus axial strain at different

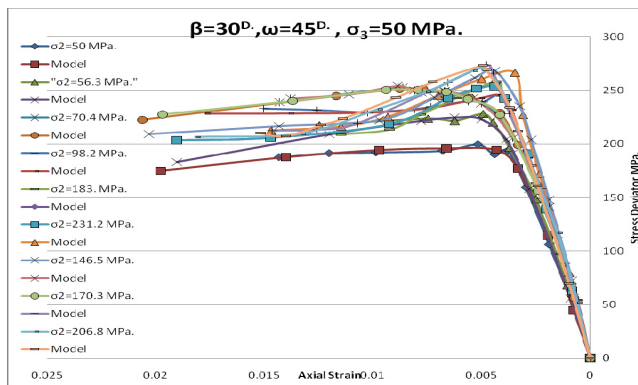


Fig. 13. Stress deviator versus axial strain at different ( $\sigma_2$ )

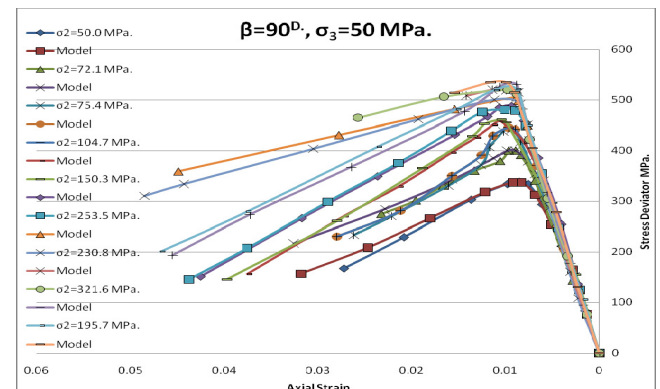


Fig. 15. Stress deviator versus axial strain at different ( $\sigma_2$ )



a metamorphic rock of porphyroblastic and fibroblastic texture and directional fabric as well as schistose structure. The rock, coming from Chichibu, Saitama Prefecture, Honshu, Japan, was characterized by planar anisotropy and the uni-axial compressive strength anisotropy coefficient  $k_c = (\sigma_c(90^\circ)/\sigma_c(30^\circ))$  equal to 2.24, with  $\sigma_c(90^\circ) = 149.6$  MPa.

More detailed data and rock sample specifications and also the mineral composition of the rock were given in (Kwasniewski & Mogi 1996) [28].

The presented comparisons show that the model has predicted comparable results as the effects of onplane shear stress axes orientation on the mechanical behavior of schistose structured rock.

Whereas the model has predicted tally results for determination of the Elasto-Plastic behavior of marble, sandstone, Quartz mica and the behavior of orientation changes in anisotropic structured schist rock samples. Therefore, it can be used to predict the Elasto-Plastic behavior of any rock with different potential of cracking.

## 9. Conclusion

Upon the presented multi-plane framework and pro-elasticity formulation, a simple relation between force/displacements on any contact plane, which thus requires fewer material parameters, led to predict anisotropic behavior of rocks. A multi-plane based model incorporating the pro-elasticity hypothesis and five typical damaged planes was developed for the elasto-plastic with different potential of cracking behavior of rocks. This model at the worst case of anisotropy needs 13 sets of parameters for different orientations in material. The main feature of this model is that it is capable of predicting the Elasto-Plastic behavior of rock without the classic plasticity formulation. Aside from modeling simplicity, the pro-elasticity and damage functions approach is more realistic and any aspect such as softening, hardening, effects of bedding plane and changes in the loading orientation and on plane shear stress direction can be predicted through the change of planar parameters.

As soon as any crack initiates and starting to grow on any of 13 micro-planes, the stiffness of the plane orthogonal to the crack line gradually decreased. When the crack opening reaches to its critical value, the components of stiffness matrix related to the direction of normal to the crack are reduced to zero. There is also a possibility the whenever, the on plane loading conditions changes in such a way that existing crack starts to be closed, while the crack opening reaches to values smaller than critical crack opening, those mentioned stiffness components increase again and go back to its initial intact values.

The capability of the model to reproduce the behavior of the different rocks has been checked and demonstrated. To clarify the capability of the proposed model, the test results conducted on marble, sandstone, Quartz mica schist and anisotropic schist are produced by the model. A good accuracy was obtained between numerical simulations and experimental results.

Although the proposed model has excellent features such as pre-failure configuration of inside material, final failure

mechanism, capability of seeing induced/inherent anisotropy and also any fabric effects on material behavior, in such a case that the basis of its formulation is simple, logical and has some physical insights that make it convenient to perceive.

## References

- [1] Chang C.S, Hicher P.Y.: An elasto-plastic model for granular materials with microstructural consideration, *International Journal of Solids and Structures*, 2005, Vol. 42, pp. 4258–4277.
- [2] Drucker D.C.: A definition of a stable inelastic material. *Journal of Applied Mechanics*, 1959, Vol. 26, pp. 101–106.
- [3] Mroz Z.: Non-associated flow laws in plasticity. *Journal de Mechanique* 1963; Vol. 2, pp. 21–42.
- [4] Mroz Z.: On forms of constitutive laws for elastic–plastic solids. *Archiwum Mechaniki Stosowanej* 1966; Vol. 18, 1–34.
- [5] Mandel J.: Conditions de Stabilité et Postulat de Drucker. In: Kravichenko, J., Sirieys, P.M. (Eds.), *Proceeding of the IUTAM Symposium on Rheology and Soil Mechanics*. Springer-Verlag, Berlin, 1964, pp. 58–68.
- [6] Maier G, Hueckel T.: Nonassociated and coupled flow rules of elastoplasticity for rock-like materials. *International Journal of Rock Mechanics, Mineral Science & Geomechanics Abstract* 1979, Vol. 16, pp. 77–92.
- [7] Mogi, K. 1979. Flow and fracture of rocks under general triaxial compression. *Proc. 4th int. Congr. on Rock Mechanics*, Monireux. Vol. 3, 123-130. Rotterdam; Balkema.
- [8] Aki, K., Richards, P.G., 1980. *Quantitative Seismology*, Freeman and Co., New York. Backus, G., *Continuum Mechanics*, Samizdat Press, (<http://samizdat.mines.edu>)
- [9] Lorig, L. J., Cundall, P. A. and Hart., R. D. (1984), “Analysis of Block Test No. 1 — Inelastic Rock Mass Behavior — Phase 3 — Hexagonal, [www.winternet.com/~icg/net/rep/Cundall-rep.doc](http://www.winternet.com/~icg/net/rep/Cundall-rep.doc)
- [10] Sadri[ejad, S. A. and Labibzadeh, M., (2005), A Continuum/discontinuum Micro Plane Damage Model for Concrete, *International Journal of Civil Engineering*, Oct. 2005, vol.5, No.3, paper138.
- [11] Sadrnejad, S. A. (2006), Numerical Evaluation of Non-homogeneity and Anisotropy due to Joints in Rock Media, *International Journal of Civil Engineering*, Vol. 4, No. 2, June 2006
- [12] Batdorf SB, Budiansky B.: A mathematical theory of plasticity based on the concept of slip. *National Advisory Committee for Aeronautics*, 1949, TN 1871.
- [13] Calladine CR.: A microstructural view of the mechanical properties of saturated clay. *Géotechnique* 1971; Vol.21, No.4, pp. 391–415.
- [14] Taylor GL: Plastic strain in metals. *Journal of the Institute of Metals* 1938, 62, pp. 307–324 (Reprinted in the *Scientific Papers of G. I. Taylor* 1. Cambridge University Press: Cambridge, U.K., 1958).
- [15] Zienkiewicz OC, Pande GN.: Time-dependent multi-plane model of rocks—a numerical study of deformation and failure of rock masses. *International Journal for Numerical and Analytical Methods in Geomechanics* 1977, Vol.1, No.3, pp. 219–247.
- [16] Pande GN, Sharma KG.: Multi-plane model of clays—a numerical evaluation of the influence of rotation of principal stress axes. *International Journal for Numerical and Analytical Methods in Geomechanics* 1983, Vol.7, No.4, pp. 397–418.
- [17] Sadrnejad S.A, Pande GN.: A multi-plane model for sands. In *Proceedings of the 3rd International Symposium on Numerical Models in Geomechanics (NUMOG)*, Niagara Falls, Canada, Pietruszczak S, Pande GN (eds). Elsevier: London, 1989, pp. 17–27.
- [18] Brinkgreve RBJ, Broere W, Waterman D.: *Plaxis, Finite Element Code for Soil and Rock Analyses*, 2006; Users Manual. PLAXIS b.v. The Netherlands.

- [19] Wiltafsky Ch.: A multi-plane model for normally consolidated clay. Ph.D. Thesis, Gruppe Geotechnik Graz, Heft 18, Graz University of Technology, Austria, 2003.
- [20] Scharinger F. Schweiger HF.: Undrained response of a double hardening multi-plane model for soils. In Proceedings of the 11th International Conference of the International Association of Computer Methods and Advances in Geomechanics (IACMAG), Turin, Italy, Barla G, Barla M (eds). Patron Editore: Bologna, 2005, pp. 505–512.
- [21] Bazant, Z., B.Oh. "Micro plane model for progressive fracture of concrete and rock." J. E. Mech., 111, pp.559-582, 1985.
- [22] Bazant, Z., P. Prat. "Micro plane model for brittle plastic material: Part I & II." J. E. Mech., 114, pp.1672-1702, 1988.
- [23] Carol, I., M. Jirasek and Z. P. Bazant. "A thermodynamically consistent approach to micro plane theory. Part I: Free energy and consistent micro plane stresses." Int. J. Solids & Structures, 38, 2921-2931, 2001.
- [24] Z. P., Giovanni, D. L., 2004. Nonlocal Micro-planes Model With Strain-Softening Yield Limits. International Journal of Solids and Structures, 41, pp. 7209-7240.
- [25] Varadarajan A, Sharma K.G, Hashemi M. Strain – softening behavior of a schistose rock mass under triaxial loading. ISRM 2003-Technology roadmap for rock mechanics, South Africa Institute of Mining and Metallurgy.
- [26] Scharinger F.: A multi-plane model for soil incorporating small strain stiffness. Ph.D. Thesis, Gruppe Geotechnik Graz, Heft 31, Graz University of Technology, Austria 2007.
- [27] Kwasniewski, M. & K- Mogi 1990. Effect of the intermediate principal stress on the failure of a foliated anisotropic rock. In H.P. Rossnani (ed.). Mechanics of Joints and Faulted Rock- 407-416, Rotterdam: Balkema.
- [28] Kwasniewski, M- & K. Mogi 1996. Finding of a foliated rock in a general triaxial field of compressive stresses. Prace Naukowe UniwersyteHU gliysides0 1602:209-232.
- [29] Nakata Y, Hyodo M, Murata H, Yasufuku N.: Flow deformation of sands subjected to principal stress rotation. Soils and Foundations 1998, Vol. 38, No. 2, pp. 115-128.
- [30] Nayeri, A., Fakharian, K., 2009. Study on Pullout Behavior of Uniaxial HDPE geogrids Under Monotonic and Cyclic Loads. International Journal of Civil Engineering. Vol. 7, No. 4, pp. 211-223.
- [31] Abdi, M.R., Sadrnejad, S.A., and Arjomand, M.A., 2009. Clay Reinforcement Using geogrid Embedded In Thin Layers of Sand. International Journal of Civil Engineering. Vol. 7, No. 4, pp. 224-235.
- [32] Salehzadeh H., Hassanlourad M., Procter D. C., and Merrifield C. M., (2008) Compression and Extension Monotonic Loading of a Carbonate Sand, International Journal of Civil Engineering, Vol. 6, No. 4, December 2008.
- [33] Sadrnejad S.A. and Labibzadeh, M., (2005), A Continuum/discontinuum Micro Plane Damage Model for Concrete, International Journal of Civil Engineering, vol.5, No.3, paper138.
- [34] Sadrnejad S.A., (2006), Numerical Evaluation of Non-homogeneity and Anisotropy due to Joints in Rock Media, International Journal of Civil Engineering. Vol.4, No. 2.
- [35] Sadrnejad S.A. and Karimpour H., (2011), Drained and Undrained Sand Behaviour by Multilaminate Bounding Surface Model, International Journal of Civil Engineering, vol.9, No.2